Photoproduction of charm in the subtractive quark model

J. Pumplin
Department of Physics, Michigan State University, East Lansing, Michigan 48824
(Received 17 May 1983)

We calculate inclusive photoproduction of charm, and exclusive photoproduction of J/ψ, using a gluon-exchange model, and compare the results with experiment. Analogous reactions involving strange and bottom quarks are also calculated. Large violations of vector-meson dominance are predicted.

I. INTRODUCTION

Let us suppose that QCD is the correct theory of strong interactions. Can we use it to understand the small-momentum-transfer processes which make up the majority of hadronic interactions? This paper pursues one line of attack on that question by applying QCD perturbation theory, supplemented where necessary by phenomenological assumptions, to two processes in diffractive photoproduction. The objective is not to test the validity of QCD, but rather to test its applicability to soft diffractive processes. This applicability is open to doubt—irrespective of the correctness of QCD—because in the absence of a large momentum transfer, the QCD coupling $\alpha_s(q^2)$ is not small compared to one. On the other hand, perturbation theory has been found to produce some successful results at low q^2,[1] and it is therefore worthwhile to see how far it can be pushed.

The particular reactions considered in this paper are those of exclusive and totally inclusive photoproduction of charm: $\gamma p \to \psi p$ and $\gamma p \to c\bar{c}X$. These reactions are well constrained theoretically because the couplings of charmed quarks to the photon and to the J/ψ are known. These reactions are also of current experimental interest. The analogous reactions involving s quarks and b quarks are also calculated here.

An additional motivation for this study lies in the observation that charm photoproduction can be used to measure the gluon momentum distribution in the proton, according to the quark-gluon-fusion model.[2,3] There are significant corrections to the fusion model which result from the off-shell behavior and the transverse-momentum distributions of the virtual gluons which undergo fusion. These corrections are automatically included in the subtractive quark model, so our results should be superior to the fusion calculation.

II. THE SUBTRACTIVE QUARK MODEL

The first assumption we make is that of the Low-Nussinov model[4]: total cross sections can be calculated from single-gluon exchange. The gluon exchange leads to a separating pair of color octets, which are assumed to dress themselves into the physical hadrons of the final state with unit probability. The details of this dressing are irrelevant for calculating total cross sections and other diffractive processes.

An immediately attractive aspect of the Low-Nussinov picture is that it provides an explanation for the most obvious feature of diffractive processes: their approximately constant energy dependence. The explanation follows directly from the spin 1 of the gluon. Single-gluon exchange, as used in this paper, predicts energy dependences which are constant except for threshold effects. Higher-order corrections of a perturbative or nonperturbative[5] type may allow one to understand the slow ($\sim \log^n s$) variations which are observed in total cross sections. An investigation of these higher-order corrections to the model presented here is currently in progress.

According to our first assumption, total cross sections are generated by single-gluon exchange [Fig. 1(a)]. Amplitudes for elastic and diffractive inelastic processes follow from unitarity: their absorptive parts are given by two-gluon-exchange discontinuities, as shown in Fig. 1(b). Our second basic assumption, which was pioneered by Gunion, Soper, and Brodsky,[6] is that the two-gluon absorptive parts which appear in Fig. 1(b), can be calculated using valence-quark models for the hadrons. This assumption is implicit in Fig. 1, and is illustrated in Fig. 2 for photoproduction and in Fig. 3 for proton-proton scattering.

A crucial aspect of the gluon-exchange model is the existence of strong cancellations between the diagonal and the off-diagonal terms of Figs. 2, 3(b), and 3(c), i.e., destructive interference between the various graphs of Fig. 1(a). This follows directly from the color-singlet nature of the hadrons. It implies that hadronic total cross sections increase with the size of the hadron. Since these sizes are inversely related to the quark masses, this picture provides a simple physical explanation for familiar observations

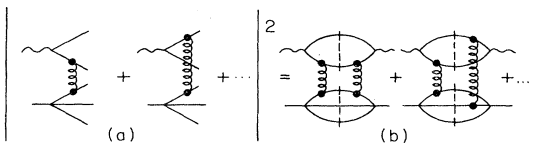

FIG. 1. (a) Low-Nussinov model for the γp total cross section. (b) The elastic amplitude it generates by unitarity. This two-gluon-exchange absorptive part is generalized to nonforward directions and the final photon is replaced by ψ to calculate the inelastic diffractive process $\gamma p \to \psi p$.

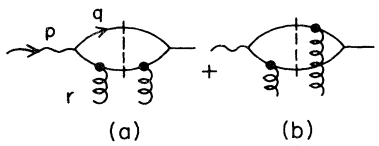

FIG. 2. (a) Diagonal and (b) off-diagonal terms in the two-gluon-exchange absorptive part for vector-meson photoproduction.

such as $\sigma_{\pi p} > \sigma_{Kp}$, which would otherwise be mysterious.

Because of the importance of color cancellations in this model, we refer to it as the subtractive quark model.[1] This term contrasts it with the pre-QCD "additive" quark model, in which quarks have internal hadronic structure and color effects are ignored.[7] It is amusing to note that the successful quark-counting predictions of the additive model, such as $\sigma_{\pi p} = \frac{2}{3}\sigma_{pp} \times$(size effect), carry over to the subtractive model. This is clear because the diagonal terms of the subtractive model correspond directly to additive terms, while the off-diagonal terms have an equal but opposite color weight since the full amplitude must vanish in the limit of zero transverse separation of the quarks.[1,8] Color cancellations also suppress higher-order corrections to one-gluon exchange, such as gluon bremsstrahlung.[9] This tends to make the one-gluon approximation plausible.

The completeness of the color cancellation depends on the transverse separations of the quarks in the beam and target particles, as well as on the overall impact parameter. The relative and overall impact parameters vary from event to event. The resulting fluctuations generate, via unitarity, a large cross section for inelastic diffraction.[10] This is a further qualitative and quantitative[1] success of the picture.

III. PROTON-PROTON SCATTERING

We begin by fitting pp scattering in the subtractive quark model. The fit requires several phenomenological assumptions. Its purpose is to obtain a parametrization of the gluon-proton absorptive part which is consistent with experiment. The calculations of photoproduction in Secs. IV and V require no further assumptions, so they provide a solid basis for testing the model against experiment.

The key objects in Fig. 3(a) are the gluon-proton absorptive parts. We derive a model for them [Figs. 3(b) and 3(c)] in a heuristic manner. Imagine for a moment that the proton couples to three spinless quarks by means of a point coupling G. In the limit of large positive longitudinal momentum, the absorptive part corresponding to Fig. 3(c) would be given by

$$\text{disc}M = g^2\delta(p_+ r_-)p_\mu p_\nu T \,, \tag{1}$$

$$T = N\int \prod_{i=1}^{3}(d^2\vec{q}_i dx_i/x_i)\delta\left[1-\sum x_i\right]\delta^{(2)}\left[\sum \vec{q}_i\right] \times (A-m_p^2)^{-1}(A'-m_p^2)^{-1} \,, \tag{2}$$

where $N = G^2/32\pi^5$ and

$$A = \sum (q_i^2+m^2)/x_i \,, \qquad A' = \sum (q_i'^2+m^2)/x_i \,, \tag{3}$$

with $\vec{q}\,'_1 = \vec{q}_1 - x_1\vec{\Delta}$, $\vec{q}\,'_2 = \vec{q}_2 - x_2\vec{\Delta} + \vec{r}$, and $\vec{q}\,'_3 = \vec{q}_3 - x_3\vec{\Delta} + \vec{\Delta} - \vec{r}$ for the particular diagram shown. The diagonal terms are given by obvious changes of $\vec{q}\,'_i$. The vectors here are transverse momenta, with $\vec{\Delta} = \vec{p}\,' - \vec{p}$. The x_i are light-cone fractions: $x_i = q_i^+/p_+$, $p_+ = p_0 + p_3$. In order to normalize the proton wave function which is implicit in this model, consider the electromagnetic form factor. It is proportional to the diagonal terms above, and is given by Eqs. (1)–(3) with $N = G^2/256\pi^6$ and $\vec{q}\,'_1 = \vec{q}_1 - x_1\vec{\Delta}$, $\vec{q}\,'_2 = \vec{q}_2 - x_2\vec{\Delta}$, and $\vec{q}\,'_3 = \vec{q}_3 - x_3\vec{\Delta} + \vec{\Delta}$. The requirement that the form factor equals 1 at $\vec{\Delta}^2 = 0$ determines the coupling G^2.

The model we use for the proton is given by Eqs. (1)–(3), except that we replace the power-law denominators $(A-m_p^2)^{-1}$, $(A'-m_p^2)^{-1}$ in Eq. (2) by exponential forms $\exp(-\beta A)$, $\exp(-\beta A')$. (Exponential factors involving the proton mass squared are absorbed into the definition of G^2.) This replaces the point coupling of the proton to quarks by a "soft" wave function, and causes the transverse momenta of the quarks to be exponentially limited. Sizable intrinsic transverse momenta can appear in the model only through QCD radiative corrections. Our use of spin-0 quarks in the proton wave function is acceptable, because their coupling to soft gluons at high momentum is the same as for spin $\frac{1}{2}$.

Our proton wave function is only used to calculate the two-gluon discontinuities of Figs. 3(b) and 3(c). It is therefore not necessary that it agree in detail with other models of the proton. In fact, however, the transverse-momentum and x distributions of the quarks turn out to be entirely reasonable.

The imaginary part of the elastic amplitude corresponding to Fig. 3(a) is given by

$$\text{Im}M = \frac{4}{(2\pi)^4}\int d^4r(\text{disc}M_{\text{beam}})(\text{disc}M_{\text{target}}) \times (r^2-\mu^2)^{-1}[(k'-k-r)^2-\mu^2]^{-1} \,. \tag{4}$$

This expression contains a factor 8 from the sum over gluon colors. The gluon propagators are modified at small momentum transfer by including a gluon mass μ to mimic confinement.[5] Results are fairly insensitive to this parameter, which we take equal to m_π. (The cross section

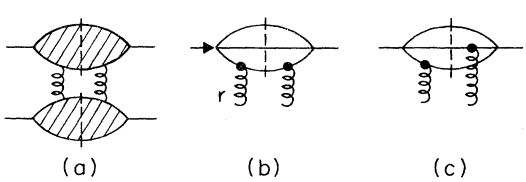

FIG. 3. (a) Low-Nussinov model for the pp elastic amplitude. (b) Diagonal and (c) off-diagonal contributions to the two-gluon-exchange absorptive part which occurs in (a).

at the very large impact parameter, which is reflected in fine details of the variation in the slope of $\log d\sigma/dt$ at small t, would reveal the effect of μ. It also affects the cross section at $s\to\infty$ at the 20% level.)

In the limit of high energy, the gluon-proton discontinuities reduce to the form

$$\text{disc}M_{\text{beam}}=(4\pi/3)g^2\delta(p_+r_-)p_\mu p_\nu T(\vec{r},\vec{\Delta})\ , \tag{5}$$

$$\text{disc}M_{\text{target}}=(4\pi/3)g^2\delta(k_-r_+)k_\mu k_\nu T(\vec{r},\vec{\Delta})\ . \tag{6}$$

The delta functions reduce Eq. (4) to a two-dimensional integral over the transverse momentum $\vec{r}$. The normalization is such that the diagonal contributions of $T(\vec{r},\vec{\Delta})$ reduce to 3=the number of constituents, at $\vec{\Delta}=0$.

The gluon coupling is momentum-transfer dependent in QCD. Hence, we replace

$$(g^2/4\pi)^2\to\alpha_s(r^2)\alpha_s((p'-p-r)^2)\ .$$

We parametrize the coupling by

$$\alpha_s(q^2)=(12\pi/25)/\ln(C+|q^2|/\Lambda^2)\ , \tag{7}$$

which corresponds to four active flavors at large q^2.

A straightforward approach at this point would be to choose the parameter β which governs the size of the proton by fitting the proton electromagnetic form factor, and to choose the nonasymptotic constants C and Λ which govern α_s to make it of order 1 at small q^2. This approach yields a prediction for pp scattering which agrees with the observed total cross section and the elastic slope at small momentum transfer within a factor of 2. This is a nontrivial success of the model, in as much as the model contains large factors like 8 from color and 2π to various powers.

In order to define the model precisely, we choose $\beta=2.0\ \text{GeV}^{-2}$, $C=3.28$, and $\Lambda=1$ GeV. These parameters produce a fit to the observed pp total cross section and the slope of elastic scattering for $0<-t<0.2\ \text{GeV}^2$ in the energy range $s=200$–$5000\ \text{GeV}^2$. The fit is accurate to better than 10% in these parameters, and the shape of $d\sigma/dt$ is good.[11]

In making the fit, the model has been "eikonalized." The process of eikonalization is expressed most simply in terms of impact parameter, where it amounts to replacing $\Omega(\vec{b})$ by $1-e^{-\Omega(\vec{b})}$, where

$$\sigma_{\text{tot}}=2\int d^2\vec{b}(1-e^{-\Omega(\vec{b})})\ . \tag{8}$$

Eikonalization is a simple way to include some effects which are due to multiple-gluon exchange. These effects are known to be present, since elastic scattering and diffractive dissociation involve ≥ 2 gluons in the amplitude and hence ≥ 4 gluons in the cross section, and yet they contribute significantly to σ_{tot}. The effect of eikonalization is to lower the pp cross section by about 20%. Eikonalization can be neglected in calculating the photoproduction amplitudes, because of the subtractive-quark-model nature of the interaction: the color-neutral $q\bar{q}$ system of heavy quarks has a very small interaction probability as a result of the color cancellations, and double scattering is therefore unimportant.

With the parameters chosen, the proton radius is approximately 20% smaller than would have been determined by fitting the electromagnetic form factors. The gluon coupling squared $\alpha_s(q^2)$ falls monotonically from 1.27 at $q^2=0$ to 0.33 at $q^2=100\ \text{GeV}^2$. The average value of q^2 which occurs in the fit to σ_{pp} is $0.6\ \text{GeV}^2$. The average value of $\alpha_s(q^2)$ is 1.1. The logarithmic behavior which is included in the parametrization (7) in accordance with asymptotic freedom is therefore not crucial to, or tested by, the fit.

Our model for the proton wave function is *ad hoc*. We have adjusted its parameters to agree with pp scattering, however, and it therefore accurately describes the proton as it is viewed in the Low-Nussinov picture as a source of soft gluons with a well-defined normalization and transverse-momentum structure. In Secs. IV and V, we derive predictions for photoproduction which require no further *ad hoc* assumptions. These predictions thus allow one to test the Low-Nussinov plus subtractive-quark-model idea. The predictions are not very sensitive to the parameters chosen for the wave function: varying the parameters changes the photoproduction prediction and the pp scattering "prediction" in about the same way.

IV. INCLUSIVE PHOTOPRODUCTION OF CHARM

The "open" photoproduction of charm in our picture is given by $\gamma p\to c\bar{c}X$ as shown in Fig. 1. The experimental signatures of this final state are missing energy due to neutrinos, or unpaired muons from charm decay. One can also measure inclusive D-meson production. This offers the advantage that the Feynman-x distribution reflects the charmed-quark distribution via quark recombination. There is also a small probability for the $c\bar{c}$ system to emerge in the form of a bound state. A calculation, in particular, of exclusive J/π production is given in Sec. V.

Calculating $\gamma p\to c\bar{c}X$ requires, in addition to the absorptive part of the proton-gluon interaction which was discussed in Sec. III, the photon-gluon absorptive part shown in Fig. 2. We assume pointlike spin-$\frac{1}{2}$ quarks of mass m and charge $\frac{2}{3}e$. In the limit of large photon momentum, taken to be in the positive-z direction, the proton-gluon absorptive part has the form of Eq. (5) with

$$T=\frac{4\alpha}{3\pi}\int_0^1 dx\int\frac{d^2\vec{q}}{\vec{q}^{\,2}+m^2}\left[\frac{(1-2x+2x^2)\vec{q}^{\,2}+m^2}{\vec{q}^{\,2}+m^2}-\frac{(1-2x+2x^2)(\vec{q}+\vec{r})^2+m^2}{(\vec{q}+\vec{r})^2+m^2}\right]\ . \tag{9}$$

The momentum transfer $\vec{\Delta}$ of Eq. (5) is zero here, and the photon-polarization vectors do not appear because only the helicity nonflip amplitude in the forward direction is needed to calculate the desired $\gamma p\to c\bar{c}X$ cross section via the optical theorem. The integration variables $\vec{q}$ and x in Eq. (9) are the transverse-momentum and light-cone-momentum fraction of one of the quarks. The two terms in the integrand come from the diagonal [Fig. 2(a)] and

off-diagonal [Fig. 2(b)] diagrams. Cancellation between these two terms at large q^2, which results from the color neutrality of the photon, makes the integral finite. At zero gluon momentum ($\vec{r}=0$), T goes to zero because of the cancellation. In this way, the apparent singularities of Eq. (4) in the limit of zero gluon mass are removed, and the insensitivity to that parameter arises.

The model for $\gamma p \to c\bar{c}X$ has now been completely defined. Its numerical evaluation is nontrivial, since there are six integration variables in Eq. (2) for the proton absorptive part, three more in Eq. (9) for the photon coupling, and two more for the gluon-transverse-momentum integral in Eq. (4). Of these, one azimuthal integral is trivial, and Eq. (9) can be evaluated in closed form by the Feynman-parameter technique. A seven-dimensional integral remains—even though we are using lowest-order perturbation theory for the interaction. The integrals were calculated by a Monte Carlo method: the computer program generated random momenta according to probability distributions which, to save computer time, were carefully chosen to mimic the actual integrand. An advantage of the Monte Carlo method is along with the integrated cross section, it easily supplies predictions, such as the Feynman-x distribution of the c quark, which are of interest experimentally. To check the Monte Carlo program, the cross section was calculated independently in the high-energy limit using a Gauss-Legendre integration technique.

In the high-energy limit, energy-momentum conservation simplifies to the form appearing in Eqs. (5) and (6). The beam particle and the state into which it fragments have a large plus component of light-cone momentum, and a negligible minus component, so the r_- component of momentum transfer vanishes. Similarly, the target particle and its fragments require $r_+=0$. Hence, the momentum transfer r is purely transverse. At finite energy, this simplification is unavailable, because energy-momentum conservation links the beam and target particles in a nontrivial way. A further complication arising at finite energy is that the light-cone integration variables x_i in Eq. (2) and x in Eq. (9) do not range over the entire interval from 0 to 1, because the quarks which emit gluons must be capable of supplying the appropriate r_+ and r_- components of momentum transfer. These complications were successfully met using the Monte Carlo method.

The cross section computed for $\gamma p \to c\bar{c}X$ is shown in Fig. 4. At moderately large energies it amounts to ~ 2—4% of the γp total cross section.[12] The predicted cross section rises sharply from threshold and continues to rise at extremely high energy. The energy dependence results principally from the energy and longitudinal-momentum contribution to the gluon propagator in Fig. 1. It is equal to

$$|t_{\min}| = r_z^2 - r_0^2 = r_+ r_- \sim \bar{M}_B^2 \bar{M}_T^2 / s \ ,$$

where $\bar{M}_B$ is a typical mass for the system into which the beam particle fragments, and $\bar{M}_T$ is the same for the target. The cross section does not become constant until s is so large that $|t_{\min}|$ is negligible compared to a typical transverse-momentum transfer squared, say 0.10 GeV^2.

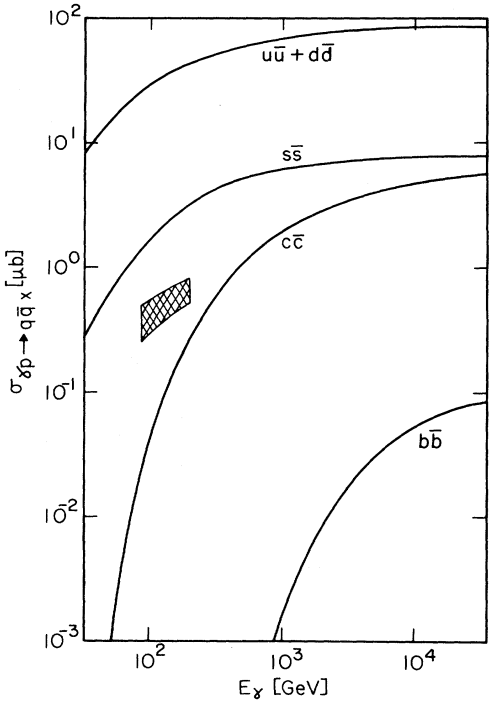

FIG. 4. Predicted cross sections for inclusive production of $b\bar{b}$, $c\bar{c}$, $s\bar{s}$, and light quarks. The shaded region shows data for $c\bar{c}$.[12]

The prediction of energy dependence at very high energies arises because there are significant contributions to the cross section from $c\bar{c}$ plane-wave states of large invariant mass.

Data for $\gamma p \to c\bar{c}p$ which have been obtained from μ^+ scattering on iron by extrapolation to $Q^2=0$ and $A=1$, using unpaired muons in the final state as a measure of D-meson decays, are also shown in Fig. 4.[12] One sees that the model calculation has approximately the correct magnitude, but an energy dependence which is somewhat stronger than is indicated by experiment. It may be that the low-energy data represents mostly nondiffractive production.

Direct measurements of $\bar{D}^0$ photoproduction at lower energy, 40—70 GeV, are consistent with pure associated production. The experimental limit $\sigma_{D^0\bar{D}^0} < 0.4\ \mu$b is consistent with the prediction in Fig. 4.[13]

Figure 4 also shows predicted cross sections for $\gamma p \to q\bar{q}X$ with $q = u+d$, s, and b. The production of b quarks is strongly suppressed by their large mass, which makes the $b\bar{b}$ system rather compact in transverse coordinate space, so that strong color cancellations take place between the diagrams of Fig. 2. The b quark is also suppressed relative to the charmed quark by a factor $\frac{1}{4}$ coming from the square of the quark charge. This same factor is present in $s\bar{s}$ production, where it makes the predicted cross section for $c\bar{c}$ almost as large as the prediction for $s\bar{s}$ at very high energy.

The prediction for $u+d$ quarks shown in Fig. 4 should not be taken too seriously, because the neglect of $q\bar{q}$ in-

teractions in the wave function of the photon is not expected to be a valid approximation for the light quarks, for which the $q\bar{q}$ separation in coordinate space is relatively large, so that confinement effects are important. Indeed, one has come to expect that the light-$q\bar{q}$ part of the photon wave function can be approximated by low-mass resonances (vector-meson dominance). It is reassuring nevertheless that the predicted cross section at high energy agrees roughly with the observed $\sigma_{\gamma p} \sim 115$ μb (for $u\bar{u}$ and $d\bar{d}$ corrected for the contributions of lower-lying Regge trajectories).[14] The energy dependence predicted in Fig. 4 for the light-quark cross section is somewhat stronger than that given by experiment. This may occur because the actual mass scale for the $q\bar{q}$ fragments of the photon is reduced from the plane-wave assumption in the model by the same $q\bar{q}$ interactions which produce the ρ resonance. Or it may be related to the discrepancy in energy dependence seen for the $c\bar{c}$ system, which is discussed in Sec. V.

The Feynman-x distribution for c or $\bar{c}$ quarks produced in $\gamma p \to c\bar{c}X$ according to the model is shown in Fig. 5. It is seen to be nearly flat in the range $0.2 < x < 0.8$. The substantial production of c quarks, and hence D mesons via dressing, with $x > 0.5$ is a key prediction of the model. The transverse-momentum distribution of the c quark varies approximately as $\exp(-1.4\,|\,\vec{q}_\perp\,|\,)$ at $s = 500$ GeV^2, and $\exp(-1.2\,|\,\vec{q}_\perp\,|\,)$ at $s = 2000$ GeV^2.

The averaged value of the gluon four-momentum squared r^2, at which the running coupling $\alpha_s(r^2)$ is evaluated is $\simeq 2$ GeV^2. For the production of the heavier-quark system $b\bar{b}$, the average r^2 (at $s = 2000$ GeV^2) is 7.2 GeV^2. This is small compared to the heavy-quark mass scale $(m_b + m_{\bar{b}})^2 \simeq 80$ GeV^2; but it is large enough that perturbation theory should work well for $\gamma p \to b\bar{b}X$ even if it does not prove adequate for $\gamma p \to c\bar{c}X$.

It is interesting to examine the extent of color cancellations in the model. If the off-diagonal terms on the proton side were omitted, the cross section would increase by 60%. If the off-diagonal terms on the proton side [Fig. 1(d)] were omitted, the cross section would increase by a factor of 25 (for $\gamma p \to c\bar{c}X$ at $s = 500$ GeV^2). The color cancellations are especially strong in this latter case because the transverse separation between quarks of mass m in the photon is small of order $\sim 1/m$.

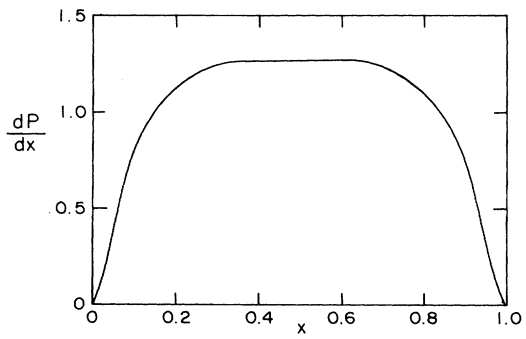

FIG. 5. Predicted distribution of longitudinal-momentum fraction for c or $\bar{c}$ in $\gamma p \to c\bar{c}X$.

V. EXCLUSIVE ψ PHOTOPRODUCTION: $\gamma p \to \psi p$

This calculation requires the $c\bar{c}$ wave function of the ψ in a Lorentz frame where it has a large momentum. One way to obtain this wave function is to solve the Schrödinger equation in the ψ rest frame, using a potential function which can be tested via the spectrum of excited states, and then boost the result to the desired frame. This boost is ambiguous, except in the extreme nonrelativistic limit in the rest frame, because the quarks are off the mass shell.

In this paper, we instead obtain a parametrization of the ψ wave function directly in the large-momentum frame, using a simple heuristic method similar to the one used for the proton in Sec. III. The method is as follows. First consider the quark loop diagram for the $\gamma\psi$ coupling [Fig. 6(a)]. Evaluate this diagram assuming a point coupling $(G/\sqrt{3})\gamma_\mu$ for the ψ to $c\bar{c}$ of a given color, making the extreme rest-frame nonrelativistic approximation $q \to k/2$ in the spin trace and closing the q^2 contour integral to obtain

$$g_{\gamma\psi} = \frac{eGm_\psi{}^2}{4\pi^3\sqrt{3}} \int_0^1 \frac{dx}{x(1-x)} \int \frac{d^2\vec{q}_\perp}{D - m_\psi{}^2} , \tag{10}$$

$$D = \frac{\vec{q}_\perp{}^2 + m^2}{x(1-x)} , \tag{11}$$

where $\vec{q}_\perp$ and x are the transverse-momentum and longitudinal-momentum fraction of the quark in a frame where the ψ has a large momentum in the longitudinal direction. To approximate the wave function in a way which simulates the effect of confinement, we replace $1/(D - m_\psi{}^2)$ by $\exp(-\gamma D/2)$ in Eq. (10). Performing the $\vec{q}_\perp$ integration leads to

$$g_{\gamma\psi} = \frac{eGm_\psi{}^2}{\sqrt{12}\pi^2\gamma} \int_0^1 dx \exp\{-\gamma m^2/[2x(1-x)]\} . \tag{12}$$

The coupling strength G is determined by the wave-function normalization. A simple way to obtain it is to imagine a ψ which is electrically charged. Its electromagnetic form factor at zero momentum transfer would equal 1, and would be given by the diagram of Fig. 6(b). Evaluating this diagram as above yields

$$1 = \frac{G^2 m_\psi{}^2}{8\pi^3} \int_0^1 \frac{dx}{x(1-x)} \int \frac{d^2q_\perp}{(D - m_\psi{}^2)^2} . \tag{13}$$

Making the exponential replacement for the energy denominator leads to

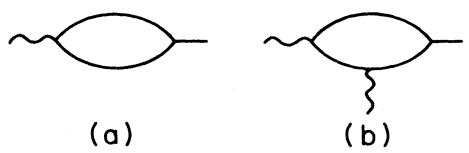

FIG. 6. Diagrams used to determine the parameters for the $\psi \to c\bar{c}$ wave function.

$$1=\frac{G^2 m_\psi^2}{8\pi^2\gamma}\int_0^1 dx\,\exp\{-\gamma m^2/[x(1-x)]\}\ . \tag{14}$$

We assume $m=m_\psi/2$. The remaining two parameters of the model are determined by the normalization condition (14) and by $g_{\gamma\psi}$ (12), which is known from the decay $\psi\to e^+e^-$:

$$\Gamma_{e^+e^-}=\frac{\alpha}{3m_\psi{}^3}g_{\gamma\psi}{}^2\ . \tag{15}$$

The parameter values are listed in Table I.

To evaluate the two-gluon-exchange absorptive parts which appear in diffractive processes we make the same set of heuristic steps as before. This should be a reasonably accurate procedure, since we have guaranteed that the effective wave function has the correct normalization and the correct value at zero $c\bar{c}$ separation. A Monte Carlo method of integration leads to the cross sections shown in Figs. 7 and 8.

The momentum-transfer dependence (Fig. 7) displays a significant amount of curvature in $\ln d\sigma/dt$ versus t. That is, the slope increases near the forward direction. The integrated cross section for $\gamma p\to\psi p$ at $E_\gamma=266$ GeV is 0.04 μb. This cross section is of course small compared with the prediction of 1.0 μb for the total charm production $\gamma p\to c\bar{c}p$, and the approximately 115 μb for $\gamma p\to$all.

The energy dependence (Fig. 8) is stronger than one might have expected for a diffractive amplitude. The large energy scale results from the energy dependences of the processes $\gamma p\to c\bar{c}qqq$ and $\psi p\to c\bar{c}qqq$, which generate the amplitude via unitarity. These processes rise slowly with energy because of their $t_{\min}$ effects, as discussed in Sec. IV.

The energy dependence of the imaginary part of the amplitude, which we calculate by unitarity, implies a real part according to analyticity. We can calculate this real part by fixed-t dispersion relations. Specifically, we require the amplitude to be an analytic function of s, with the imaginary part given by the unitarity diagrams of Fig. 1. In addition, the amplitude is an even function of s (even signature). The dispersion integral requires a subtraction for convergence: the subtraction constant is chosen by assuming the real part goes to zero as $s\to\infty$.

We calculate the real part without undertaking a full-dispersion integral calculation as follows. The energy dependence which we calculate for the imaginary part of $\gamma p\to\psi p$ is approximated quite well by the form $\exp(-s_0/s)$, where s_0 is a slowly varying function of t. The energy scale s_0 is so large, for example 180 GeV^2 at

TABLE I. Parameters which characterize the vector-meson wave functions, and the e^+e^- decay widths assumed in calculating them.

	M (GeV)	γ (GeV^{-2})	G	$\Gamma_{e^+e^-}$ (keV)
ϕ	1.0196	2.109	54.8	1.26
ψ	3.097	0.581	61.3	4.80
Γ	9.460	0.143	436.3	1.20

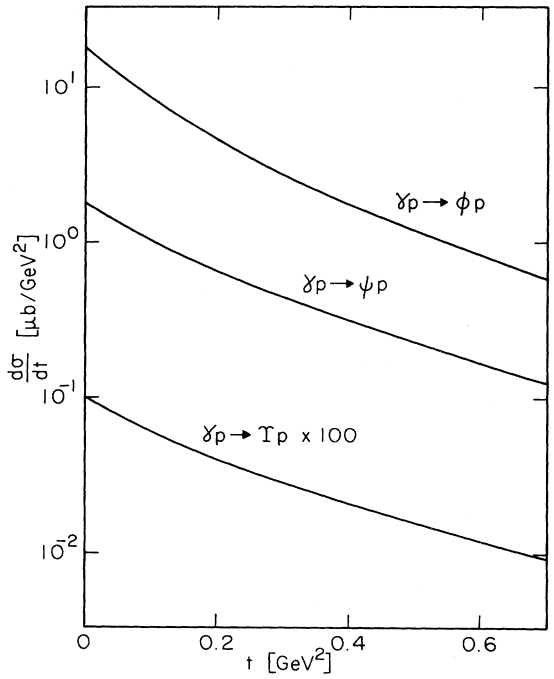

FIG. 7. Predicted momentum-transfer dependence for diffractive photoproduction at $s=500$ GeV^2.

$t=0$, compared to the physical threshold at $(m_p+m_\psi)^2=16$ GeV^2, that the form $\exp(-s_0/s)$ may reasonably be used all the way down to $s=0$. The even-signature amplitude which has an imaginary part of this form is given by a certain exponential integral, which is

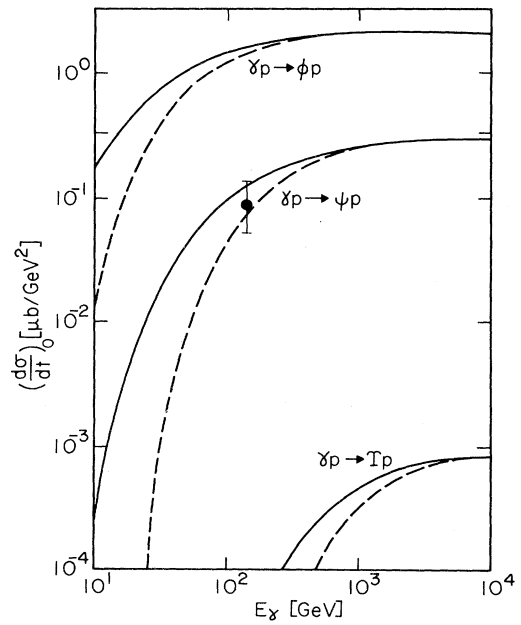

FIG. 8. Predicted energy dependence for diffractive photoproduction in the forward direction. The dashed curves show the contribution due to the imaginary part of the amplitude alone; the solid curves include the real part. The data point for $\gamma p\to\psi p$ is from Ref. 16; further data are discussed in the text.

not difficult to evaluate.

As shown in Fig. 8, we make the perhaps surprising prediction that the $\gamma p \to \psi p$ amplitude is mainly *real* at energies below $E_\gamma \sim 100$ GeV. It would be very interesting to measure this real part experimentally, as could be done via interference between leptonic decay of the ψ and pure QED (Bethe-Heitler) production of e^+e^- or $\mu^+\mu^-$.[15]

A measurement of forward $\gamma p \to \psi p$ at 140 GeV is shown in Fig. 8.[16] The agreement with experiment is good. Measurements of the integrated cross section for $\gamma p \to \psi p$ in the same experiment have smaller error bars. They show a strong rise with energy which is comparable to that predicted by the model. The absolute values are close, but are not within the experimental-error limits. For example, at photon energies of 70, 130, and 190 GeV, the model predicts cross sections of 16, 30, and 38 nb, while the observed values are 12 ± 2, 18 ± 3, and 25 ± 5 nb.

Measurements of $\gamma p \to \phi p$ also show a rise with energy,[17] which is in line with the prediction of the model but perhaps a bit more gradual. The absolute values of the cross section do not agree very well; but this is not surprising, because our simple model for the vector-meson wave function is not expected to be accurate for light mesons. At representative photon energies of 35, 71, and 157 GeV, the model predicts $\sigma_{\gamma p \to \phi p} = 130$, 209, and 270 nb, while experiment gives 510 ± 90, 650 ± 90, 650 ± 70, and 740 ± 90 nb.

VI. FAILURE OF VECTOR-MESON DOMINANCE

Previous approaches to vector-meson photoproduction have been based on the hypothesis of vector-meson dominance (VMD).[18] According to that hypothesis, the amplitude for $\gamma p \to \psi p$ is equal to $g_{\gamma\psi}/m_\psi{}^2$ times the elastic amplitude $\psi p \to \psi p$. The photon-meson coupling $g_{\gamma\psi}$ is measured by the decay rate $\psi \to e^+e^-$. The elastic amplitude is related to $\sigma_{\psi p}$ in the forward direction via the optical theorem. In order to make a nontrivial prediction, one assumes that $g_{\gamma\psi}$ and $\sigma_{\psi p}$ do not vary between the ψ mass shell and the photon mass shell.

The VMD hypothesis cannot be tested experimentally, because $\sigma_{\psi p}$ is unmeasured. (Once upon a time it was believed that $\sigma_{\psi p}$ could be determined from the A dependence of photoproduction on nuclei. This is now known to be incorrect on theoretical grounds.[19])

The VMD hypothesis can be tested theoretically using the subtractive quark model, which provides a detailed dynamical model for the amplitudes $\gamma p \to \psi p$ and $\psi p \to \psi p$. We find $\sigma_{\psi p} = 10$ mb at very high energy, and the amplitude for $\gamma p \to \psi p$ is smaller than the VDM value by a factor of 0.31 in the forward direction. (Previous calculations which were not based on gluon exchange have predicted violations of simple VDM by a factor ~ 0.5.[7,20] Of course any result can be "fit" by VDM if the $\gamma\psi$ coupling is allowed to vary with q^2.) For the other vector mesons, we calculate $\sigma_{\Upsilon p} = 3$ mb with $\gamma p \to \Upsilon p$ smaller than VDM by 0.21, and $\sigma_{\phi p} = 24$ mb with $\gamma p \to \phi p$ smaller than VDM by 0.36 in amplitude.

In our model, $\sigma_{\phi p}$ is nearly as large as the observed $\sigma_{\pi p}$. This prediction may be approximately correct, even though the ϕ meson is too light for our quasi-nonrelativistic approach to the wave function to be quantitatively accurate. It comes about because the ϕ and the π are of about the same size, and the total cross sections are generated by the exchange of gluons, which couple equally to all flavors. Our prediction for $\sigma_{\phi p}$ disagrees strongly with the prediction $2\sigma_{Kp} - \sigma_{\pi p}$ of the additive quark model. Although $\sigma_{\phi p}$ cannot be measured because of the short ϕ lifetime, measurements of total cross sections for baryons which contain strange quarks *have* been found to be inconsistent with the additive quark model.[21]

VII. CONCLUSION

Our main results are quantitative predictions for $\gamma p \to c\bar{c}X$ and $\gamma p \to \psi p$. These reactions offer a clean opportunity to test the Low-Nussinov hypothesis that diffractive processes can be described by single-gluon exchange together with unitarity. The comparison with available data is encouraging. (To test the *theoretical* consistency of the hypothesis, one could ask whether the next-order diagrams are negligibly small. An investigation of this is currently underway.) We also calculate the corresponding reactions involving s and b quarks. The s quark is too light for our model to be reliable, and in fact the quantitative results for ϕ production do not agree well with experiment. The b-quark reactions would be ideal theoretically, but have not been measured experimentally. One of the difficulties experimentally is that the cross sections are expected to be small, as predicted in Fig. 4 and 8.

We predict a rather gradual rise of the cross sections with energy, which results from the $t_{\min}$ associated with the gluon exchanges in Fig. 1. These $t_{\min}$ effects persist to high energies for which the overall $t_{\min}$ of the reaction $\gamma p \to \psi p$ is completely negligible. The energy dependence generates large real-part effects at moderate energies via dispersion relations. The $t_{\min}$ effect [in Fig. 3(a)] also makes σ_{pp} rise with energy in our model. As a result, we were able to fit the cross section tolerably well over the range $s = 200$—5000 GeV^2. At higher energies, the model cross section ceases to rise, and hence one must look beyond one-gluon exchange to understand the continued gradual rise which is observed in σ_{pp}. The energy dependences which we predict for heavy-quark production (Figs, 4 and 8) are much more dramatic than those found for σ_{pp}, however, so those predictions should be at least approximately reliable.

Our model for open-charm production is similar in spirit to a calculation by King, Donnachie, and Randa.[22] However, they neglect the finite-energy effects which we find to be important for $E_\gamma \lesssim 1000$ GeV, and do not calculate the absolute normalization of the cross section. Our model for inclusive production is different from the photon-gluon-fusion approach,[2] because in that approach the soft-gluon distribution from the target proton is obtained from the deep-inelastic structure function. The γ-g-fusion approach suffers from the fact that the gluon structure function is rather poorly known—especially at $x \simeq 0$ which is the operative region, since in the absence of a high-$P_\perp$ trigger most of the cross section comes from $c\bar{c}$-invariant masses which are fairly close to threshold. Also, there is no clear way to de-evolve the structure func-

tion to small Q^2. One might of course hope to use the γ-g-fusion model to extract the structure function from experiment. However, the model leaves out the off-shell behavior of the gluon propagator which we find to be important in the subtractive-quark-model approach. In the subtractive quark model, the gluon distribution is obtained from a model of the proton wave function, whose parameters have been adjusted to give a gluon distribution which fits the closely related process of pp elastic scattering. The gluon-propagator and color-cancellation effects are included directly. A further advantage of our approach is that it allows calculation of the exclusive process $\gamma p \to \psi p$ without making unpleasant assumptions. From an experimental standpoint, the fusion approach has so far been found to be consistent with electroproduction data.[12] We have not calculated the full range of experimental distributions, but the cross section in the subtractive quark picture fits the high-energy data at about the same level of accuracy.

Our model for exclusive photoproduction of heavy vector mesons takes the opposite viewpoint from the vector-meson-dominance approach: the photon couples initially to a noninteracting $q\bar{q}$ system rather than to the ground state of that system. We predict sizable violation of VMD. These violations cannot be observed directly, because the vector-meson elastic-scattering amplitudes are unknown.[19] One could approach them indirectly, however, by measuring coherent photoproduction on nuclear targets, and calculating those processes using the techniques of this paper.

The methods used in this paper could also be used to calculate the inclusive reactions $\gamma p \to \psi X$ and $\gamma p \to \psi' X$ which have been measured at Fermilab.[23] They could also be used to calculate the dependence on the virtual-photon mass in electroproduction, and the spin-density matrices in vector-meson production.

The magnitude of a hadron-hadron total cross section in the subtractive quark model depends upon the color distribution in the hadrons, and upon the strength of the gluon coupling to color. The color distribution is normalized in an absolute way to the number of valence quarks.[1,6,8] The strength of the gluon-quark coupling which is required to fit hadronic total cross sections using this normalization is characterized by $\alpha_s \simeq 1$. In the case of a $c\bar{c}$ system, the valence-quark model is a relatively sound assumption. The approximate agreement with experiment which we find for the photoproduction of charm therefore confirms both the validity of the model for the color distribution in the proton and the value $\alpha_s \simeq 1$ at low q^2.

ACKNOWLEDGMENT

This work was supported in part by the National Science Foundation.

[1] J. Pumplin and E. Lehman, Z. Phys. C 9, 25 (1981).
[2] J. Babcock, D. Sivers, and S. Wolfram, Phys. Rev. D 18, 162 (1978); M. Glück, and E. Reya, Phys. Lett. 83B, 98 (1979); E. Berger and D. Jones, Phys. Rev. D 23, 1521 (1981); J. Körner, *et al.*, Phys. Lett. 114B, 195 (1982); J. Leveille and T. Weiler, Nucl. Phys. B147, 147 (1979); V. Barger *et al.*, Phys. Lett. 91B, 253 (1980).
[3] T. Weiler, Phys. Rev. Lett. 44, 304 (1980).
[4] F. Low, Phys. Rev. D 12, 163 (1975); S. Nussinov, Phys. Rev. Lett. 34, 1286 (1975).
[5] A. White, Argonne National Laboratory Report No. ANL-HEP-CP-82-29, 1982 (unpublished).
[6] J. Gunion and D. Soper, Phys. Rev. D 15, 2617 (1977); S. Brodsky and J. Gunion, Phys. Rev. Lett. 37, 402 (1976).
[7] J. Pumplin and W. Repko, Phys. Rev. D 12, 1376 (1975), and references contained therein.
[8] H. Lipkin, Phys. Lett. 116B, 175 (1982).
[9] J. Gunion and G. Bertsch, Phys. Rev. D 25, 746 (1982).
[10] J. Pumplin, Phys. Rev. D 8, 2899 (1973); J. Pumplin and H. Miettinen, *ibid.* 18, 1696 (1978).
[11] U. Amaldi and K. Schubert, Nucl. Phys. B166, 301 (1980).
[12] J. Aubert *et al.*, Nucl. Phys. B213, 31 (1983).
[13] D. Aston *et al.*, Phys. Lett. 94B, 113 (1980).
[14] D. Caldwell *et al.*, Phys. Rev. Lett. 40, 1222 (1978).
[15] The phase of $\gamma C \to \phi C$ has been measured by this technique at low energy: H. Alvensleben *et al.*, Phys. Rev. Lett. 27, 444 (1971). The real part is found to be fairly small, as one expects because of the nuclear target.
[16] J. Aubert *et al.*, Nucl. Phys. B213, 1 (1983).
[17] R. Egloff *et al.*, Phys. Rev. Lett. 43, 657 (1979); D. Aston *et al.*, Nucl. Phys. B172, 1 (1980).
[18] T. Bauer *et al.*, Rev. Mod. Phys. 50, 261 (1978).
[19] H. Miettinen and J. Pumplin, Phys. Rev. Lett. 42, 204 (1979).
[20] D. Sivers *et al.*, Phys. Rev. D 13, 1234 (1976).
[21] S. Biagi *et al.*, Nucl. Phys. B186, 1 (1981).
[22] S. King, A. Donnachie, and J. Randa, Nucl. Phys. B167, 98 (1980).
[23] M. Binkley *et al.*, Phys. Rev. Lett. 48, 73 (1982); 50, 302 (1983).